

Assessment of parameters affecting H-type wind turbine performance

*Pedro Antonio Assad Baracat¹⁾ and Kamal Abdel Radi Ismail²⁾

^{1), 2)} *Energy Department, Faculty of Mechanical Engineering, UNICAMP
Campinas 13083-860, Brazil*

¹⁾ *Instituto de Pesquisas Eldorado, Campinas 13083-898, Brazil*

¹⁾ pedroaab@gmail.com ²⁾ kamal@fem.unicamp.br

ABSTRACT

Due to the drastic effects of global warming and the eminent depletion of fossil fuels in future years, worldwide efforts are being expended to include renewable energy sources of dominated technologies in the energy matrices and intensify research and development of other promising sources. Solar and wind energy appear at the top of the list of well dominated technologies of reasonable implantation and energy generation costs. The horizontal axis wind turbines are well developed and many wind farms are operating in many countries supplying clean energy for the populations. On the other hand vertical axis wind turbines are not widely acceptable, few installations are in operation and their contribution in the low power range is insignificant. Different predicted behaviors of H-type vertical axis wind turbines, produced by changing the design and environmental variables were investigated using a low computational effort algorithm developed during this study. Among the input variables are the airfoil section, chord length, wind velocity, tip speed ratio, as well as the rotor solidity, radius, height and number of blades. Simulation parameters were also varied, including the initial guess for the axial induction factor and maximum number of iterations. The outputs of the numerical code include the wind extracted power, power coefficient, thrust, thrust coefficient, torque and torque coefficient. The power coefficient defines the aerodynamic efficiency of the rotor and the fluctuations of thrust and torque reflect the force balance, indicating the level of mechanical stress over the structure. Numerical simulations and performance predictions are important, since they may reduce the need of field tests, which are usually hard and costly to perform.

Symmetrical NACA airfoils present good and similar balance of forces, with power coefficients that can exceed 0.30. At winds of 10 m/s, a 2 m radius and 4 m height rotor having 3 NACA 0012 blades with 0.67 m chord and tip speed ratio of 4.1 presents a power coefficient of 0.28 and delivers 2.7 kW of power. The level of unbalance is 46% (torque) and 76% (thrust), which may be acceptable. A high output power is due to the high wind velocity, rotor height and radius, and does not notably influence the power coefficient. More blades increase the balance, but decrease the power coefficient. The solidity and the tip speed ratio are important parameters that may be used for the power coefficient optimization.

¹⁾ Graduate Student

²⁾ Full Professor

1. INTRODUCTION

Recently, the interest in the improvement of vertical axis wind turbines (VAWTs) has been increasing. This wind turbine has its rotation axis perpendicular to the wind flow (Fig. 1), while the horizontal axis wind turbine (HAWT) has its rotation axis parallel to the wind flow (Fig. 2). Projects addressed to large-scale Darrieus VAWTs (D-VAWTs) became more frequent in the 1970s, while the H-type VAWT (H-rotor) research only became more significant during the 2010's (Möllerström *et al.*, 2019), regardless of the fact that H-rotors have simpler geometries than D-VAWTs. Actually, both lift-driven types were conceived by Darrieus in the 1920s, and the difference between them is that the H-type VAWT carries straight blades, while the D-VAWT carries curved blades. The development gap between these two types of rotors is not the only time discrepancy to be noticed in the history of VAWTs. As mentioned, the H-rotor and the D-VAWT concepts came from the 1920s. In the same decade, Savonius conceived a drag-driven type of VAWT (Savonius VAWT or S-VAWT). This represents a 50-year gap in the VAWT's research history.

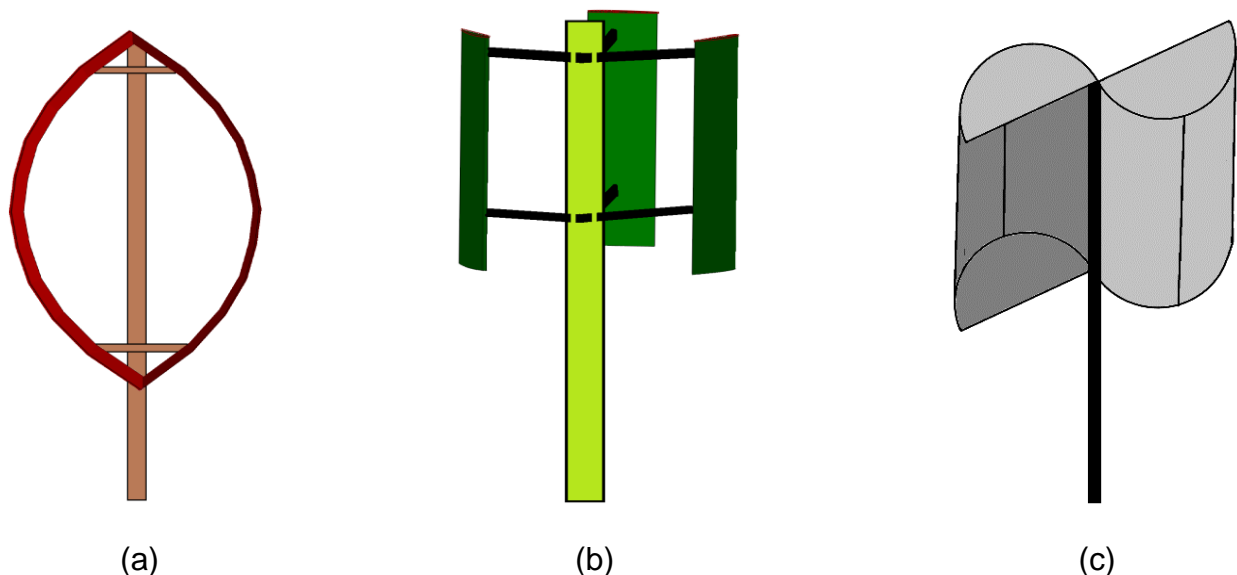


Fig. 1 Geometries of different VAWTs: (a) D-VAWT; (b) H-type VAWT; (c) S-VAWT.

At the same time as VAWT research and development were slowly conducted, the design of HAWTs was the aim of most studies related to wind energy. As a consequence, another gap was created, separating the knowledge stages of well-developed HAWTs from VAWTs. In spite of the recent studies directed to VAWTs, this gap persists, suggesting the high potential of VAWTs yet to be explored. This potential may cover higher levels of efficiency in wind energy conversion and power generation.

In order to promote significant advances in this research area, it is necessary to improve the methods of performance prediction of a VAWT to be applied in a particular environment, since they may reduce the need of hard and costly field tests, limiting them to fewer cases. Those methods should be capable to provide a reliable relation between the design parameters and their effects on the VAWT performance. While the

methodology applied for HAWTs is more consolidated, due to the stronger efforts directed to it in a longer period of time, physical aspects are responsible for the need of a more complex methodology to be applied to VAWTs. Those aspects are consequences of the complex geometry and the technical features of environments that are typical for VAWT utilization.

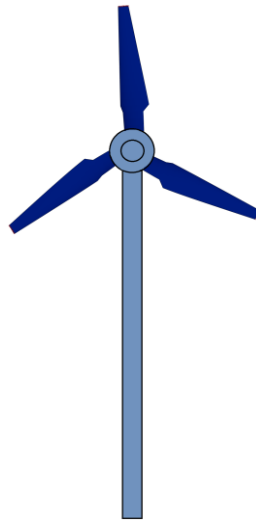


Fig. 2 HAWT geometry

The complex geometry of a VAWT results in more interactions between the air flow and the rotor blades. The air crosses the blades two times, entering at the core and leaving it. The flow at the core is disturbed by the first passage through the blades, creating a complex behavior that needs to be taken into account at the second passage. Moreover, the asymmetry of thrust produced at opposite points of the rotor creates unbalanced forces, which causes mechanical stresses in the VAWT's structure.

The typical environments for VAWTs utilization may present some limitations that usually make HAWTs utilization unsuitable on them. Among those limitations, the available space and the regularity of land relief are noticeable. Since VAWTs require less space than HAWTs, they became more common in urban spaces to low-power local energy production. While HAWTs present a good performance at flat surfaces with few obstacles, they may significantly lose efficiency in non-regular surfaces, such as mountains reliefs and building areas, which disturb the air flow in low heights. On the other hand, VAWTs are more robust to flow disturbance, making them feasible at those spaces. The flow disturbance turns the behavior prediction of a VAWT more complicated. Hence, the knowledge on how the VAWT's design and environmental parameters affect its performance is important to reduce the complexity of prediction methods.

Computational Fluid Dynamics (CFD) methods are widely used to accurately predict the efficiency of wind turbines. Some particular-case studies suggested that the refinement level of CFD simulation parameters, such as grid and azimuthal angle/time increment, have an important impact on results, but this conclusion cannot be generalized (Rezaeiha *et al.*, 2017). In a first analysis, the refinement may be used as a

way of reduce the computational effort, which reduces the simulation time. As a sophisticated tool, CFD simulations may require high levels of computational effort. Rezaeiha *et al.* described a set of 110 CDF simulations, taking about 120 hours each, performed in a 24-core supercomputer for a small-scale VAWT (Rezaeiha *et al.*, 2017). Taking into account the high cost to perform field tests on VAWTs, CFD simulations usually produce the best results, but they may be also costly to perform. Less sophisticated alternatives may reduce the computational effort and generate good results as well.

Han *et al.* reported a computational time from the order of seconds in a VAWT simulation, using an improved the double-multiple stream tube (DMST) model, against 3 to 4 hours using the 3D vortex panel method on a single Intel Core 2 processor (Han *et al.*, 2014). The DMST is a simpler method in which the numerical modelling is more directly connected to the analytical modeling. As a result, it could be expected a pattern in the influences of VAWT parameters on the results. On the other hand, some aerodynamic effects may be neglected, leading to less accurate results. However, they still may be considered good or acceptable when compared to other methods, especially for the study of a rotor with simple geometry. In other words, it is possible to achieve good results through a simple algorithm that requires low computational effort, in which the input parameters maintain a standard relation with the results. This method may present better results for an H-rotor, as its simple geometry may contribute for a less disturbed flow pattern, which fits better on assumptions and hypotheses of the theory.

The purpose of this paper is to evaluate the influences of H-type VAWT's design, environment and simulation variables on the performance prediction, through a simple method of low computational effort. It is based on the momentum theory and stream tubes (ST) models. Some important input parameters are the constant blade chord, solidity, airfoil shape, rotor radius, rotor height, number of blades, lift and drag coefficients for different Reynolds numbers/angles of attack, tip speed ratio (TSR) range and free stream wind velocity. The lift and drag coefficients were obtained experimentally at Sandia National Laboratories and are available in the literature for symmetrical NACA airfoils (Sheldahl *et al.*, 1981), and may carry some aerodynamic effects and losses that may help to achieve better results. However, the data on lift and drag coefficients for a range of angles of attack covering 360° are scarce and often need interpolation.

Important results are the produced power, power coefficient and thrust curves for different values of TSR. The power prediction is important to verify if the VAWT is potentially capable to supply its future demand. The power coefficient reflects the aerodynamic efficiency of the rotor. Even with a high power production, a low power coefficient means that the potential for wind energy production is higher than the delivered energy. Furthermore, the power and power coefficient are the last outputs calculated in the algorithm, carrying previous calculations. Hence, they are good results to be used in the method validation process. The thrust curve provide maximum, minimum and average values in one revolution. The difference between the maximum and minimum values over the maximum value gives a percentage that reflects the VAWT balance. High values indicate unbalance of forces, leading to high-level of mechanical stresses over VAWT's structure. The TSR is a variable that can be set on

the VAWT design. Therefore, it is desirable to obtain values that lead to optimum results for different operating conditions.

2. METHODOLOGY

2.1 Code

In order to produce a simple and reliable computational algorithm, the analytical modelling was translated into a numerical Matlab code, composed by the momentum theory and an enhanced single stream tube (SST) model, with experimental results for the lift coefficient (C_l), and drag coefficient (C_d). The enhanced SST model considers the two phases of the flow crossing the H-rotor, and its simplifying hypotheses are compensated by the experimental data used, which carries neglected effects.

The TSR was considered as a design parameter. The angular velocity (ω) may be chosen instead of TSR, however both are linked by the free stream velocity (V_∞) and constant rotor radius (R), as described by Eq. (1).

$$TSR = \frac{\omega R}{V_\infty} \quad (1)$$

The first iterative process is based in the TSR variation, with increments of 0.1. For each TSR iteration, the rotor is analyzed in a full rotation, at each blade. As a reference, the azimuthal angle of first blade (θ) leads another iteration process, with increments of 1° . Finally, the code proceeds to the calculation of the induction factor (a), as described by Fig. 3. From the calculated values of the induction factor, it is possible to calculate the instant local flow velocity at the core (V_c) and the downstream velocity (V_d), as in Eq. (2) and Eq. (3) (Biadgo *et al.*, 2012).

$$V_c = V_\infty(1 - a) \quad (2)$$

$$V_d = V_\infty(1 - 2a) \quad (3)$$

From the flow velocity at the core, the instant local angle of attack (α) is obtained through Eq. (4) (Biadgo *et al.*, 2012).

$$\alpha = \frac{V_c \sin \theta}{V_c \cos \theta + \omega R} \quad (4)$$

The convergence of the induction factor is based on the comparison of two calculated values of instant local thrust (T), described by Eq. (5) and Eq. (6) (Biadgo *et al.*, 2012).

$$T = 0.5\rho V_r^2 Hc(C_n \sin \theta - C_t \cos \theta) \quad (5)$$

$$T = 2\rho Aa(1-a)V_\infty^2 \quad (6)$$

Where C_t is the instant local tangential force coefficient, described by Eq. (7), C_n is the instant local axial force coefficient, described by Eq. (8) (Biadgo *et al.*, 2012), ρ is the air density, V_r is the instant local velocity over the airfoil, described by Eq. (10), H is the rotor height, c is the chord and A is the swept area of the rotor.

$$C_t = C_l \sin \alpha - C_d \cos \alpha \quad (7)$$

$$C_n = C_l \cos \alpha + C_d \sin \alpha \quad (8)$$

Two different values of instant local thrust coefficient (C_T) may be calculated using Eq. (7) and Eq. (8) on Eq. (9).

$$C_T = \frac{T}{0.5\rho V_\infty^2 A} \quad (9)$$

Since the lift and drag coefficients are given in tables for a set of angles of attack, and each table corresponds to a particular Reynolds number (Re), the code perform a search on those tables, in order to find the table with the closest instant Reynolds number. However, it is necessary to compute the instant Reynolds number, which depends on the instant local velocity over the airfoil, as estimated by Eq. (10).

$$V_r = \sqrt{\left(\omega R + \frac{V_i + V_d}{2} \cos \theta\right)^2 + \left(\frac{V_i + V_d}{2} \sin \theta\right)^2} \quad (10)$$

Where V_i is either the free stream velocity or the downstream velocity, depending on the azimuthal angle. If the azimuthal angle is equal or lower 180° , the upwind part of the rotor is being analyzed. Hence, V_i assumes the free stream velocity value. If the azimuthal angle is higher than 180° , the downwind part of the rotor is being analyzed. In this case, V_i assumes the downstream wind velocity value. The instant local Reynolds number can be calculated through Eq. (11).

$$Re = \frac{\rho V_r c}{\mu} \quad (11)$$

Where the local chord of the airfoil was constant for each H-rotor analyzed in this paper. The solidity (σ) is another important variable, that depends on the number of blades (N), as defined in Eq. (12).

$$\sigma = \frac{Nc}{2R} \quad (12)$$

As an alternative to reduce the computing time, an average Reynolds number

may be estimated at the beginning of the simulation, taking into account the symmetry of the rotor and its average angular velocity ($\bar{\omega}$), which can be calculated from the TSR interval to be analyzed. Eq. (13) describes the average Reynolds number.

$$\text{Re} = \frac{\rho \bar{\omega} R c}{\mu} \quad (13)$$

The instant local lift (L) and drag (D) forces can be calculated using the rotor height (H), through Eq. (14) and Eq. (15).

$$L = 0.5 C_{l_i} \rho V_r^2 c H \quad (14)$$

$$D = 0.5 C_{d_i} \rho V_r^2 c H \quad (15)$$

Assuming the same format of Eq. (7), the instant local tangential force (F_T) is calculated through Eq. (16).

$$F_T = L \sin \alpha - D \cos \alpha \quad (16)$$

From the tangential force, it is possible to calculate the instant local torque (Q), power (P) and power coefficient, as in Eq. (17), Eq. (18) and Eq. (19).

$$Q = F_T R \quad (17)$$

$$P = \omega Q \quad (18)$$

$$C_p = \frac{P}{P_{wind}} \quad (19)$$

In Eq. (19), P_{wind} is the power contained in the wind, calculated through Eq. (20).

$$P_{wind} = 0.5 \rho A V_{\infty}^3 \quad (20)$$

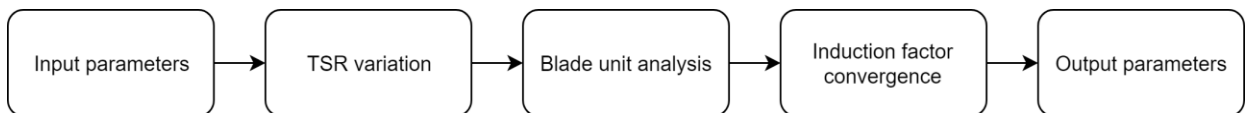


Fig. 3 Algorithm block diagram

2.2 Parameters Variation

Table 1 shows the standard geometric and environmental variables for the simulations. The parameters were changed from those standards individually. In some cases, changing one parameter may force another change, as is the case of solidity and chord. For the same, number of blades and rotor radius, changing the solidity

values cause the change of the chord. The most noticeable results are discussed ahead.

Table 1: Standard variables

Rotor radius (m)	2
Chord (m)	0.67
Solidity	0.5
Rotor height (m)	04
Number of blades	3
Airfoil	NACA 0012
Air density (kg/m ³)	1.2047
Air dynamic viscosity (kg/(m.s))	0.000018205
TSR range	0.1 – 9.0
TSR sample	2
Free stream velocity (m/s)	4

3. VALIDATION

In order to validate the method, an H-rotor with the same geometry as a literature sample was simulated. In this case, mechanical and electrical efficiencies were considered, in a value of 0.9 together. The environment conditions were also reproduced from the same source, as indicated in Table 2 (Kumar *et al.*, 2017).

Table 2: Validation rotor and simulation parameters

Rotor radius (m)	0.2
Chord (m)	0.1
Solidity	0.43
Rotor height (m)	0.3
Number of blades	3
Airfoil	NACA 0018
Air density (kg/m ³)	1.2047
Air dynamic viscosity (kg/(m.s))	0.000018205
TSR range	0.1 – 2.0
Free stream velocity (m/s)	12

The last result to be computed is the power coefficient. It depends on most previous calculations. Hence, the power coefficient is the best result to use for comparison purposes. Fig. 4 shows the compared results, which will be discussed in the next section.

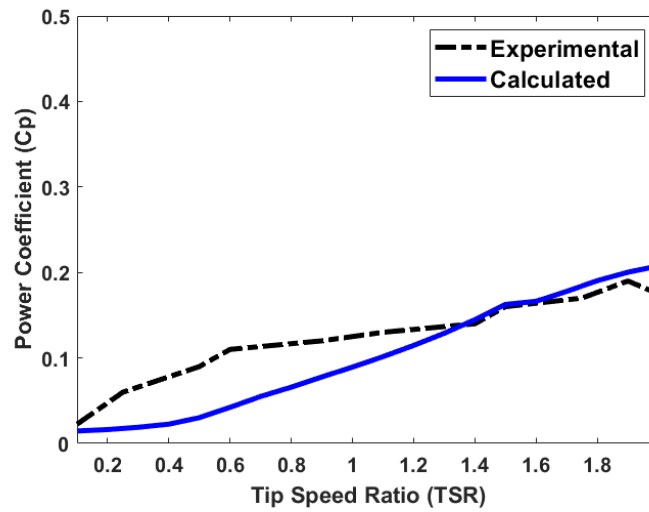


Fig. 4 Power coefficients versus tip speed ratios (experimental and calculated) (Kumar *et al.*, 2017)

4. RESULTS

4.1 Free Stream Velocity Variation

The free stream velocity was simulated as 2, 4 and 10 m/s. They did not show significant variation in their results, except for the produced power and force unbalance. Higher free stream velocities led to higher output power values, from 9 W at 2 m/s and to 68 W at 4 m/s to 1004 W at 10 m/s, for a TSR of 1 (Fig. 5). The force unbalance also increased from 40% at 2m/s and 4 m/s to 76% at 10 m/s. Since higher free stream velocities carry higher amounts of power, it is expected higher output power, thrust and unbalance values. However, there is a limit for it, which is not taken into account in a simple calculation.

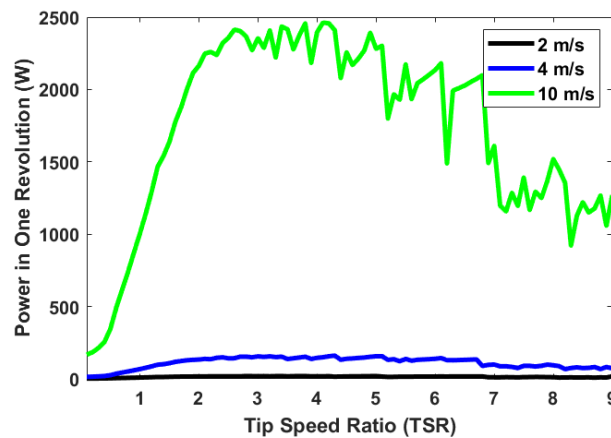


Fig. 5 Total power (one revolution) for free stream velocities of 2 m/s, 4 m/s and 10 m/s

4.2 Rotor Radius and Height Variation

A larger rotor radius also increased the output power (Fig. 6) and unbalance, from 34 W and 41% with 1 m radius to 169 W and 75% with 5 m radius (TSR of 1), without considerable impacts at other results. The power coefficient presented a small change from 0.12 with 1 m radius to 0.11 with 5 m radius, at a TSR of 1, which were not the maximum values in both curves.

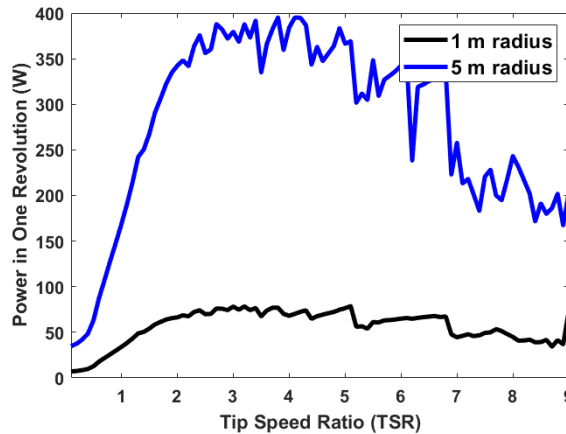


Fig. 6 Total power in one revolution for 1 m rotor radius and 5 m rotor radius

The same effect in output power was observed increasing the rotor height from 1 m to 8 m (Fig. 7), At 1 m height, the output power was 17 W against 135 W at 8 m height, for a TSR of 1. At the same TSR, the power coefficient maintained its value of 0.11, as well as the force unbalance of 40%.

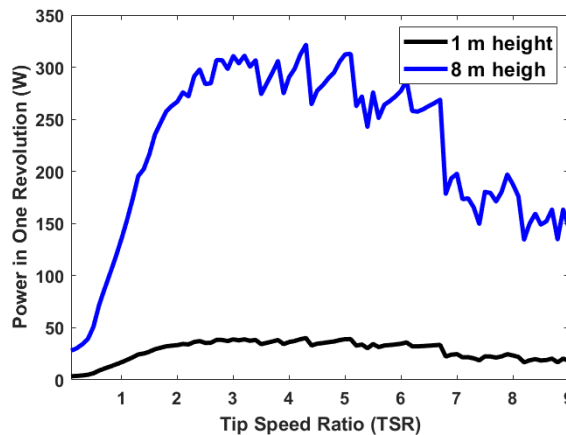


Fig. 7 Total power in one revolution for 1 m rotor height and 8 m rotor radius

Higher values of radius and height produce higher values of output power as well, since they increase the crossing flow area. In other words, more wind is captured by the rotor. As a consequence, more power is captured as well.

4.3 Number of Blades Variation

Changing the number of blades from 2 to 4 and 10 produced a high impact on power and power coefficient curves with TSR, as well as thrust with time curves (Fig. 8 and Fig. 9).

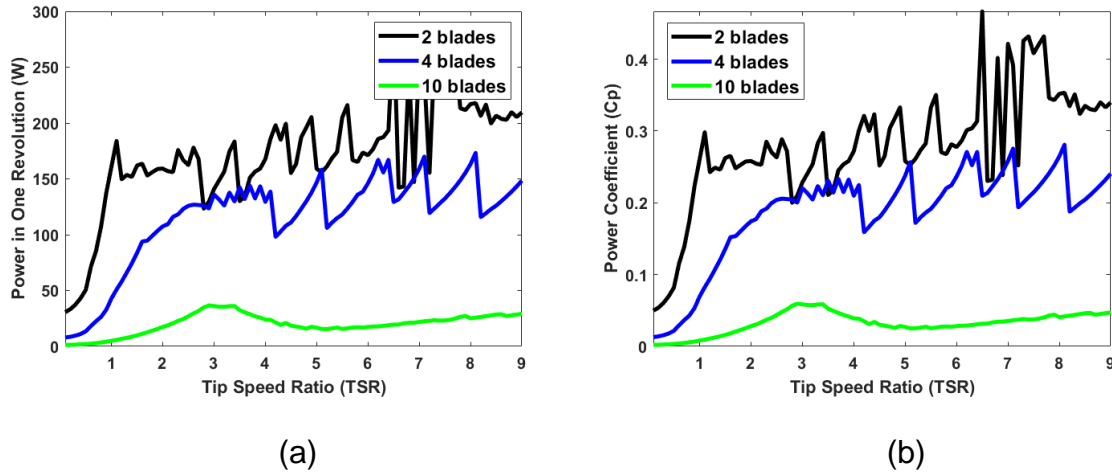


Fig. 8 (a): Total power in one revolution versus tip speed ratio; (b): Power coefficient in one revolution versus tip speed ratio - 2, 4 and 10 blades

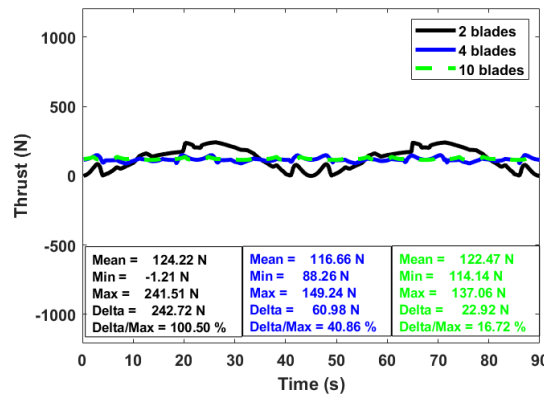


Fig. 9 Total thrust in versus time in one revolution - 2, 4 and 10 blades

In order to maintain the same solidity of 0.5, the chord values changed. For a TSR of 1, it was observed a power of 161 W with 2 blades, 43 W with 4 blades and 5 W with 10 blades. The power coefficient was 0.26 with 2 blades, 0.07 with 4 blades and 0.008 with 10 blades (TSR of 1 as well). The force unbalance was 100% for 2 blades, 41% for 4 blades and 17% for 10 blades.

The effect of the number of blades in the results is a parameter that is well represented by this simple method. A rotor with low number of blades usually present a higher power coefficient and produces more power, since the flow disturbance at the core is reduced. However, the rotor also loses its capability of maintaining balance,

leading to more mechanical stresses.

From Fig. 8, it is possible to deduce that the results may not maintain a well behaved pattern for TSR values higher than 4, which is a limitation of the present method.

4.4 Solidity Variation

The effect of solidity in the results was observed during this work. Simulations showed that higher solidity values may cause a slight growth in power and power coefficient values. However, the unbalance level may also grow slightly (Fig. 10 and Fig. 11). For a solidity of 0.2 and TSR of 1, the output power was 27 W and the power coefficient was 0.04. For a solidity of 0.5 and TSR of 1, the output power was 68 W and the power coefficient was 0.11. For a solidity of 0.9 and TSR of 1, the output power was 109 W and the power coefficient was 0.2. The unbalance level was 39% for a solidity of 0.2, 40% for a solidity of 0.5 and 53% for a solidity of 0.9.

The solidity tends to have a great influence in the results. However, the slight changes observed may be explained by the type of rotor, in which the straight blades tends to reduce the influence of solidity. Another reason may be a limitation of actuator disc theory as well.

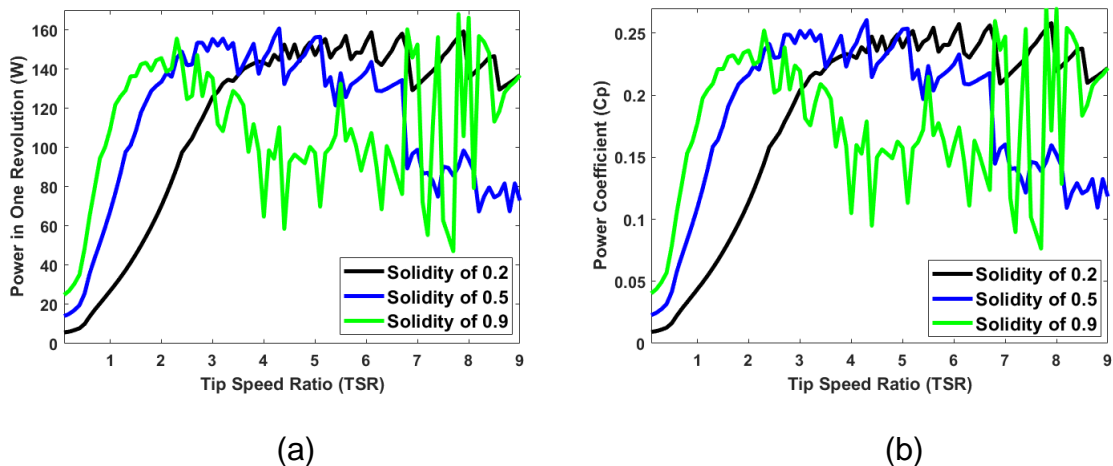


Fig. 10 (a): Power in one revolution versus tip speed ratio; (b): Power coefficient versus tip speed ratio - solidity of 0.2, 0.5 and 0.9

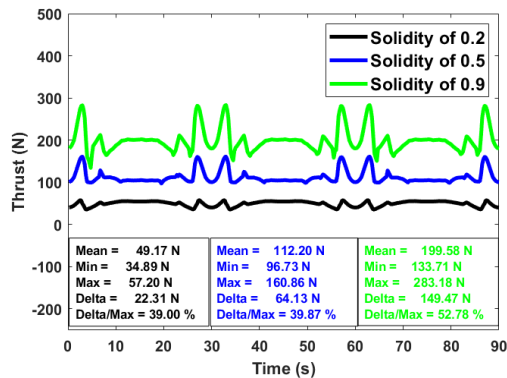


Fig. 11 Full thrust versus time in one revolution - solidity of 0.2, 0.5 and 0.9

4.5 Airfoil Variation

Symmetrical NACA airfoils such as NACA 0012, NACA 0015 and NACA 0018 presented similar results, with about 68 W of output power (as reproduced by Fig. 12) and 0.11 of power coefficient for a TSR of 1. The force balance maintained a level close to 39% in all cases. The performance reduced significantly for non-symmetrical airfoils, circular arc airfoils and flat plates.

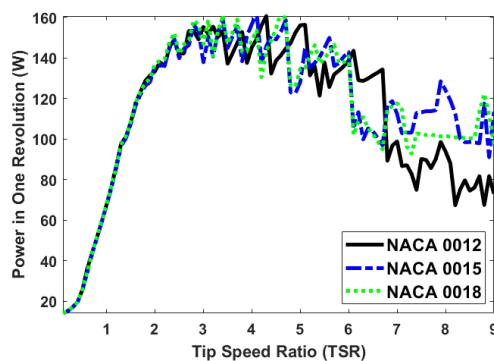


Fig. 12 Power in one revolution versus tip speed ratio - NACA 0012, NACA 0015 and NACA 0018

Symmetrical airfoils like the NACA 0012, NACA 0015 and NACA 0018 tends to produce similar results, since their shapes are also similar. Even so, small differences could be seen by using the present method. Other airfoils like the NACA 4412 and the S809 are non-symmetrical and may not be suitable for the use in VAWTs. The flat plate and the circular arc airfoil could perform well in a VAWT. However, it is necessary to perform simulations under different parameters.

5. CONCLUSIONS

This paper have successfully described the influence of several geometric and environmental parameters on the performance prediction of H-type VAWTs.

It was investigated the influence of the rotor radius, height, number of blades and chord/solidity on the produced power, power coefficient and force balance of straight-bladed Darrieus VAWTs, as well as the free stream velocity, tip speed ratio and Reynolds number estimation in the same outputs.

Parameters of high influence were the number of blades, rotor radius, height and free stream velocity, as expected. It was expected a higher influence of the solidity than occurred, which may indicate the need of future work on the method, in order to add new mathematical relations that reproduce well that influence.

Considering the high number of simulations, a fast computing method was essential to reach the presented results, which may not be as realistic as those produced by sophisticated methods, like CFD, but are not far behind them. As suggested by the observation of the effects of solidity on results, future work may produce a high-fidelity method based on this, without increasing the computational effort.

It is important to repeat the same procedures of this work, aiming to establish a better knowledge base for VAWTs, in order to better promote more researches and spread its use around the world.

ACKNOWLEDGMENT

The first author wishes to thank the *Instituto de Pesquisas Eldorado* (Eldorado Research Institute) for the financial support.

The second author wishes to thank the *Conselho Nacional de Desenvolvimento Científico e Tecnológico* (CNPq) for the PQ Research Grant.

The authors thank the Faculty of Mechanical Engineering (FEM) and the State University of Campinas (Unicamp) for providing the necessary additional structure used during the period of this work.

REFERENCES

- Biadgo, A.M., Simonovic, A., Komarov, D. and Stupar, S. (2013), "Numerical and analytical investigation of vertical axis wind turbine", *FME Transactions*, **41**, 49-58.
- Han, Y., Sitaraman, J. and Dan, Y. (2014), "Analysis of vertical axis wind turbine aerodynamics by using a multi-fidelity approach", *Annual Forum Proceedings - AHS International*, **3**, 2101-2111.
- Kumar, P.M., Rashmitha, S.R., Srikanth, N. and Lim, T.-C. (2017), "Wind tunnel validation of double multiple streamtube model for vertical axis wind turbine", *Smart Grid and Renewable Energy*, **8**, 412-424.

- Möllerströma, E., Gipeb, P., Beurskensc, J. and Ottermoa, F. (2019), "A historical review of vertical axis wind turbines rated 100 kW and above", *Renewable and Sustainable Energy Reviews*, **105**, 1–13.
- Rezaeihaa, A., Montazeria, H. and Blockena, B. (2018), "Towards accurate CFD simulations of vertical axis wind turbines at different tip speed ratios and solidities: Guidelines for azimuthal increment, domain size and convergence", *Energy Conversion and Management*, **156**, 301–316.
- Sheldahl, R.E. and Klimas. P.C. (1981), "Aerodynamic characteristics of seven symmetrical airfoil sections through 180-degree angle of attack for use in aerodynamic analysis of vertical axis wind turbines", *Sandia National Laboratories, Energy Report, SAND80-2114*.